JOURNAL OF APPLIED ELECTROCHEMISTRY 21 (1991) 457–462

The hydrogen evolution reaction in an acid medium on nickel electrodeposited with $PMo_{12}O_{40}^{3-}$ or MoO_4^{2-}

O. SAVADOGO*, S. LÉVESQUE

Département de Génie Métallurgique, École Polytechnique de Montréal, C.P. 6079, succ. "A", Montréal, Québec. H3C 3A7, Canada

Received 24 July 1990; revised 7 September 1990

Nickel was electrodeposited from dilute aqueous solutions of nickel chloride, containing MoO_4^{2-} or $PMo_{12}O_{40}^{3-}$ ions. It was shown that improvement in the overpotential (η) and in the exchange current density (i_0) of the electrodes depends on the composition of the deposition bath. The h.e.r. electrocatalytic activity of the electrodeposits was then analysed and related to their chemical composition. The results show that some extremely active electrocatalysts are produced when combinations of nickel–molybdenum (Ni–Mo) are formed. The influence of the MoO_4^{2-} or $PMo_{12}O_{40}^{3-}$ concentration in the electrode deposition electrolyte on the electrocatalytic properties of these deposits for the hydrogen evolution reaction (h.e.r.) was investigated. The effects of the deposition current density on the electrocatalytic properties of the electrodes were also studied. The best electrocatalytic properties for the h.e.r. were obtained with electrodes electrodeposited with 2 g dm^{-3} of MoO_4^{2-} or $PMo_{12}O_{40}^{3-}$. The kinetic parameters for the h.e.r. in H_2SO_4 1 M were deduced for temperatures ranging from 298 to 378 K.

1. Introduction

Studies to date relating to the analysis of the hydrogen evolution reaction on electromodified electrodes may be summarized as follows: on the electrocatalytic properties of electrodes the surfaces of which have been modified by heteropolyacids (HPAs) [1–5]; on the basic concepts of the Brewer theory of intermetallic phases [6–8] and on typical issues arising from the electrocatalytic activity achieved as a function of the composition of hypo–hyper-d-electronic transition metals [9]. It has been shown that the bulk properties of these intermetallic phases determine their electrocatalytic activity for the hydrogen evolution reaction (h.e.r.). This reaction has also been performed with Chevrel-type cluster compounds [10]. The remixed cluster compounds were found to be the best electrodes for the h.e.r. (Both intermetallic systems of hypo–hyper-d-electronic metal combinations and cluster materials were prepared thermally.)

In previous papers [11–15], we have shown that electrodeposited nickel electrodes modified by heteropolyacids (HPAs) provide good electrocatalytic properties for the h.e.r. in an acid medium. A detailed study was carried out to investigate how HPAs influence the electrocatalytic properties of the electrodeposited electrodes for the h.e.r. A significant decrease in overpotential (η) and an increase in exchange current density (i_0) were observed. A nickel electrode prepared with $SiMo_{12}O_{40}^{4-}$ in an acetate bath was found to be a better electrocatalyst than platinum for the h.e.r. in an acid medium [15]. This may be attributed to the production of an extremely active Ni–Mo electrocatalyst when a synergetic activation d-metal (Ni) is combined with a reactivity-inductive d-metal (Mo). It was also found that the HPA-modified electrodeposited nickel electrode is less sensitive than platinum to impurity effects for the h.e.r., while tin and lead impurities in the nickel significantly alter the characteristics of the electrode [13]. The effect of the concentration of $SiW_{12}O_{40}^{4-}$ on the electrocatalytic properties of these deposits and its influence on the h.e.r. have also been investigated. Nickel electrodeposited with a concentration of 8 g dm^{-3} of $SiW_{12}O_{40}^{4-}$ was, in fact, found to exhibit the best electrocatalytic parameters for this reaction [13, 15].

This report deals with the electrocatalytic behaviour of nickel electrodeposited on a stainless steel cathode from baths containing either $PMo_{12}O_{40}^{3-}$ or MoO_4^{2-}. The electrolyte in each of the baths contained the same chemical constituents except for the heteropolyacid. How these different heteropolyacids affect the electrocatalytic parameters of the electrodes was analysed.

2. Experimental procedure

2.1. *Electrodeposition*

All the chemicals used were reagent grade (Fisher Scientific, BDH or Anachemia) except for the H_3BO_3, $NiCl_2 . 6H_2O$ and the dodecyl sodium sulphate. The cathode used in the electrodeposition process was

* To whom correspondence should be sent.

0021-891X/91 $03.00 + .12 © 1991 Chapman and Hall Ltd.

316 stainless steel (Firth Brown Inox Ltd) with a 1 cm × 2 cm surface area, and the anode was a sheet of nickel (99%) of surface area 5 cm × 5 cm.

Prior to electrodeposition, the electrodes were degreased and cleaned with acetone and HNO_3. They were then activated by anodic electrochemical polishing for 20 min in 1 M H_2SO_4 at a current density of 35 mA cm^{-2} using a Hewlett Packard (Model HP6266B) power supply.

The electrodeposition of the electrodes was performed using the same power supply (HP 6266B) at different cathodic current densities (i_d). The electrodeposition baths were prepared with distilled water. The heteropolyacid concentration was within the optimum range previously used in the successful electrodeposition of nickel from chloride baths [11–15]. The reproducibility of the process was checked at least 10 times for each electrode, and the results were found to be completely reproducible. Electrodes were also prepared from electrolytes containing various concentrations of $PMo_{12}O_{40}^{3-}$ or MoO_4^{2-} in the base solution. Concentrations of 1, 2, 4 and 8 g of $PMo_{12}O_{40}^{3-}$ or MoO_4^{2-} per litre (dm^3) of base electrolyte were used. The nickel electrodes electrodeposited with $PMo_{12}O_{40}^{3-}$ were identified respectively as $NilPMo_{12}$, $Ni2PMo_{12}$, $Ni4PMo_{12}$ and $Ni8PMo_{12}$. The nickel electrodes electrodeposited with MoO_4^{2-} were labelled respectively NilMo, Ni2Mo, Ni4Mo and Ni8Mo. The electrodeposition process lasted 6 h. The reproducibility of the process was checked at least 10 times for each electrode. The results were found to be completely reproducible. The reproducibility of the electrocatalytic parameters (h.e.r. exchange current density, Tafel slope and hydrogen overvoltage) of the electrodes was also checked in assessing the overall reproducibility of the electrodeposition process.

2.2. *Electrochemical equipment and electrodes*

The cathode polarization of the electrodeposited electrodes was measured using a PAR (Model 273) potentiostat and monitored by PAR Universal Programmer software (Model 342). Reagent grade H_2SO_4 was used for the cathodic polarization studies of the h.e.r. The solutions were deoxygenated thoroughly with nitrogen, and kept under a positive pressure with this gas throughout the experiment. The polarization curves were obtained using a single-compartment cell with a standard three-electrode configuration. The reference electrode was a saturated calomel electrode (SCE), the counter electrode was platinum gauze with a large surface area and the working electrode was an electrodeposited electrode with a geometric area of 2 cm^2. All experimental results were referenced to this apparent geometric surface area, which may possibly differ to some extent from the real surface area of the samples. As other investigators have pointed out [16], the real surface area on an "atomic level", particularly in the case of porous or rough electrodes (like the electrode investigated here), cannot be determined experimentally with certainty. Therefore, a discussion of electrocatalytic effects based on the real surface area was not considered. Since some measurements on rotating disc electrodes do not show any convection effects on the polarization curves, all the results presented here were obtained using stationary electrodes. In order to ensure the reproducibility of the results, each experiment was performed at least three times.

3. Results and discussion

3.1. *Effect of* $[PMo_{12}O_{40}^{3-}]$ *or* $[MoO_4^{2-}]$

Figure 1 shows the typical quasi steady-state polarization curves obtained on electrodeposited nickel with different concentrations of $PMo_{12}O_{40}^{3-}$ under potentiodynamic conditions at the low sweep rate of 2 mV s^{-1}. As may be seen, at a constant potential in the region of the hydrogen evolution reaction (h.e.r.), the current density (i_c) of the nickel electrodeposited with $[PMo_{12}O_{40}^{3-}]$ is more significant than that of the nickel electrodeposited without $[PMo_{12}O_{40}^{3-}]$. It may also be seen that in a large domain of this region (h.e.r.), the curves exhibit typical Tafel behaviour.

The Tafel lines for the h.e.r. indicate that the electrocatalytic activity of the nickel electrodeposited with different concentrations of $PMo_{12}O_{40}^{3-}$ or MoO_4^{2-} is much better than that of the electrodes electrodeposited without $PMo_{12}O_{40}^{3-}$. Analogous results are obtained with electrodes electrodeposited with MoO_4^{2-}. The variation of i_0 with $[PMo_{12}O_{40}^{3-}]$ or $[MoO_4^{2-}]$ is reported in Fig. 2. As may be seen, there is a remarkable variation in the exchange current density of the h.e.r. $[PMo_{12}O_{40}^{3-}]$ or $[MoO_4^{2-}]$. The results show that the i_0 values of the h.e.r. on the electrodes electrodeposited with $[PMo_{12}O_{40}^{3-}]$ or $[MoO_4^{2-}]$ are greater than the i_0 value of the h.e.r. on nickel electrodeposited without

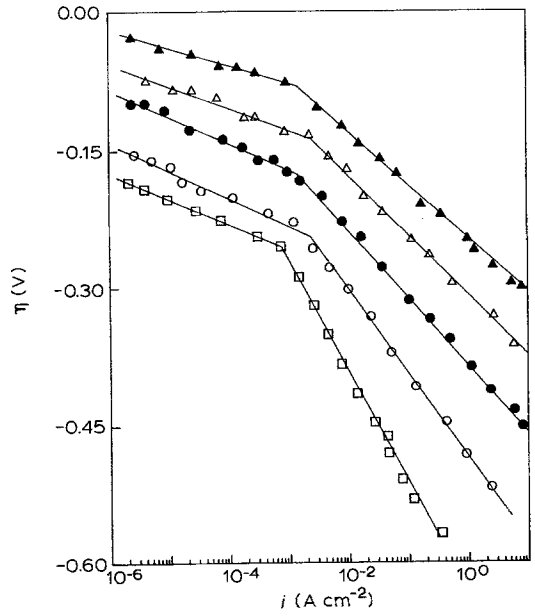

Fig. 1. Quasi steady-state polarization curves for the h.e.r. obtained under potentiodynamic conditions at a low sweep rate of 2 mV s^{-1} in 1 M H_2SO_4 at 298 K: (□) Ni, (○) $Ni8PMo_{12}$, (●) $NilPMo_{12}$, (△) $Ni4PMo_{12}$ and (▲) $Ni2PMo_{12}$.

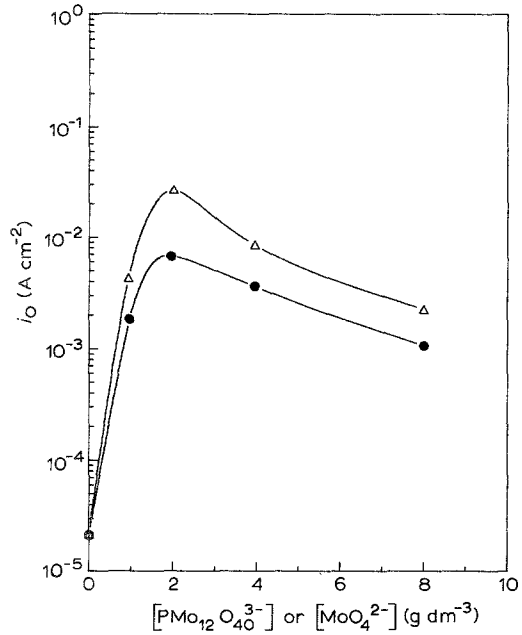

Fig. 2. Variation of the exchange current density of the hydrogen evolution reaction (i_0) in 1 M H_2SO_4 at 298 K of nickel electrodeposited at 35 mA cm^{-2}. (●) Nickel electrodeposited with $[PMo_{12}O_{40}^{3-}]$, (○) nickel electrodeposited with $[MoO_4^{2-}]$.

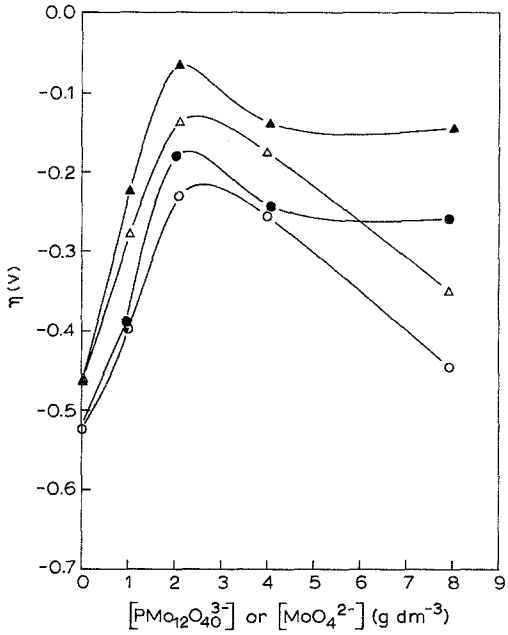

Fig. 3. Variation of the hydrogen overvoltage (η) in 1 M H_2SO_4 at 298 K of nickel electrodeposited at 35 mA cm^{-2}. (○, ●) Nickel electrodeposited with $[PMo_{12}O_{40}^{3-}]$ with η at 0.5 A cm^{-2}; (△, ▲) nickel electrodeposited with $[MoO_4^{2-}]$ with η at 0.1 A cm^{-2}.

these species (see Fig. 2). In particular, the maximum values of i_0 are obtained for Ni2PMo$_{12}$ and Ni2Mo$_{12}$ (see Fig. 2). On the other hand, the i_0 value of Ni2PMo$_{12}$ is smaller than that of Ni2Mo$_{12}$ (9×10^{-3} A cm^{-2} against 6×10^{-2} A cm^{-2}). However, with the addition of different concentrations of $PMo_{12}O_{40}^{3-}$ or MoO_4^{2-} the electrodeposited nickel with MoO_4^{2-} has a higher exchange current density than that fabricated with $PMo_{12}O_{40}^{3-}$. Thus, the increase in i_0 value is related to the effect of $PMo_{12}O_{40}^{3-}$ or MoO_4^{2-}. On the other hand, the h.e.r. overvoltage changes with $[PMo_{12}O_{40}^{3-}]$ or $[MoO_4^{2-}]$ (see Fig. 3). The lowest overvoltage is obtained with an electrode fabricated with 2 g dm^{-3}. It has also been observed that the lowest Tafel slopes were obtained when the electrodes were produced with 2 g dm^{-3} of $[PMo_{12}O_{40}^{3-}]$ or $[MoO_4^{2-}]$ (see Table 1). The different results also indicate that the Ni/Mo electrodes are better electrocatalysts for the h.e.r. than the Ni/PMo$_{12}$ electrodes. This may be attributed to the electrocatalytic activation of the proton reduction by the electrodeposited nickel electrode. In particular, the change in the electrocatalytic properties for the electrodeposited nickel with different concentrations of $PMo_{12}O_{40}^{3-}$ or MoO_4^{2-} can be linked to the nature of the reduced compounds of $PMo_{12}O_{40}^{3-}$ or MoO_4^{2-} produced during the electrodeposition process. Support for this conclusion may be found by determining the chemical composition of the electrodes. Figures 4 and 5 show the X-ray fluorescence spectroscopy (XRFS) analysis of the electrodes. Nickel, molybdenum and phosphorus are detected in electrodes fabricated with $PMo_{12}O_{40}^{3-}$, while nickel and molybdenum are detected in electrodes fabricated with MoO_4^{2-}. Using the height of the XRFS peak of each component in the diagram, the relative Mo/Ni and P/Ni ratios are shown in Table 2. As may be seen, the Mo/Ni ratio for electrodes fabricated with 2 g dm^{-3} of $PMo_{12}O_{40}^{3-}$ or MoO_4^{2-} is greater than those of the other electrodes. On the other hand, the P/Ni ratio does not change with different concentrations of $PMo_{12}O_{40}^{3-}$. Thus, the decrease in the hydrogen overvoltage and the increase in the h.e.r. exchange current density for the electrodeposited nickel with different concentrations of $PMo_{12}O_{40}^{3-}$ or MoO_4^{2-} can be linked to the presence of

Table 1. H.e.r. Tafel slope at 298 K in 1 M H_2SO_4 for nickel electrodeposited with $PMo_{12}O_{40}^{3-}$ or MoO_4^{2-} at 35 mA cm^{-2}

Compound	Ni	Ni1PMo$_{12}$	Ni2PMo$_{12}$	Ni4PMo$_{12}$	Ni8PMo$_{12}$	Ni1Mo	Ni2Mo	Ni4Mo	Ni8Mo
b (mV dec^{-1})	140	120	80	100	100	110	70	80	100

Table 2. Mo/Ni peak (Pr) ratio deduced from X-ray fluorescence spectroscopy of nickel electrodeposited with $[PMo_{12}O_{40}^{3-}]$ or $[MoO_4^{2-}]$ at 35 mA cm^{-2}

	Ni1Mo	*Ni2Mo*	*Ni4Mo*	*Ni8Mo*	*Ni1PMo$_{12}$*	*Ni2PMo$_{12}$*	*Ni4PMo$_{12}$*	*Ni8PMo$_{12}$*
Pr (Mo/Ni)	0.5	5	3	2	0.2	3	1	0.5
Pr (P/Ni)	0	0	0	0	0.8	0.75	0.9	0.85

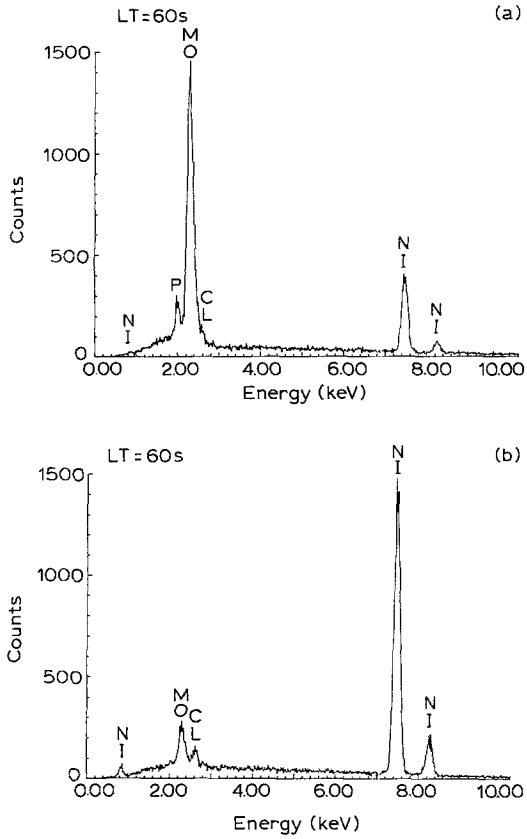

Fig. 4. X-ray fluorescence spectroscopy analysis of the electrodes: (a) $Ni2PMo_{12}$; (b) $NilPMo_{12}$.

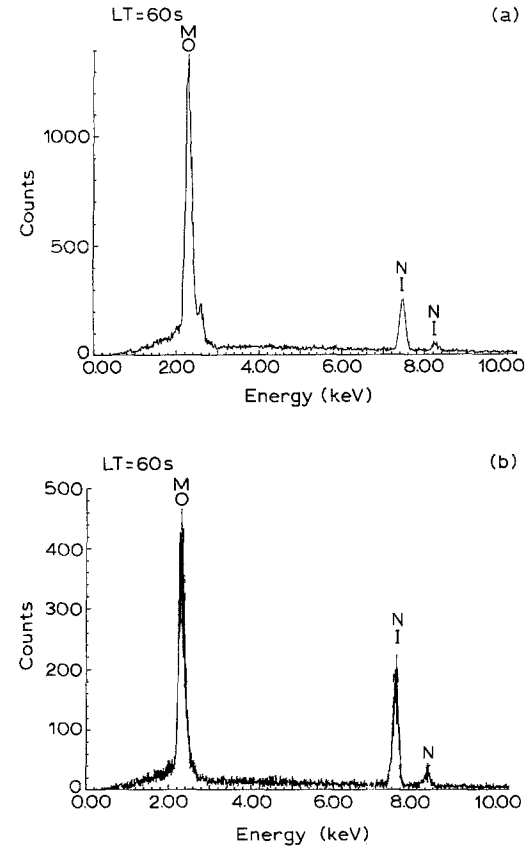

Fig. 5. X-ray fluorescence spectroscopy analysis of the electrodes: (a) Ni2Mo; (b) Ni8Mo.

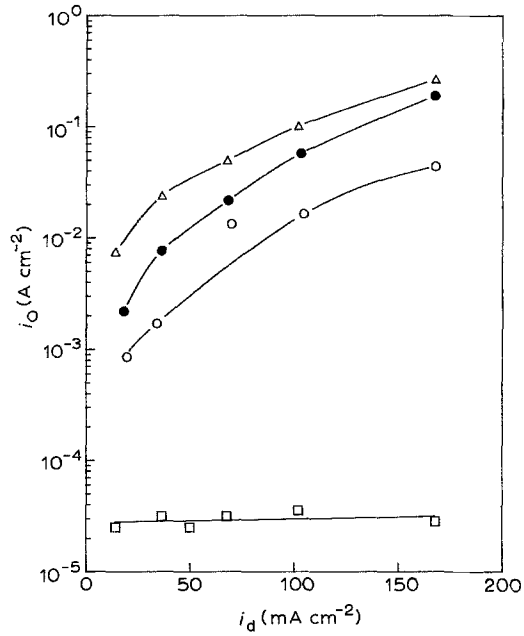

Fig. 6. Variation of the h.e.r. exchange current density in 1 M H_2SO_4 at 298 K with the electrodeposition current density of several electrodes: (□) Ni, (○) $Ni8PMo_{12}$, (●) $Ni2PMo_{12}$, and (△) Ni2Mo.

molybdenum in the electrodes. Support for this conclusion may be found by studying the effect of the electrodeposition current density (i_d) on the exchange current density (i_0) and the hydrogen overvoltage (η). The variation of (i_0) and (η) with i_d when nickel is electrodeposited with and without $PMo_{12}O_{40}^{3-}$ or MoO_4^{2-} is shown in Figs 6 and 7. As may be seen, i_0 and $|\eta|$ do not change with i_d for electrodes fabricated without $PMo_{12}O_{40}^{3-}$ or MoO_4^{2-}, whereas i_0 increases and $|\eta|$ decreases with i_d for electrodes electrodeposited with $PMo_{12}O_{40}^{3-}$ or MoO_4^{2-}. The Mo/Ni and P/Ni ratio peaks are shown in Table 3 for different values of i_d. As may be seen, Mo/Ni increases with i_d, whereas

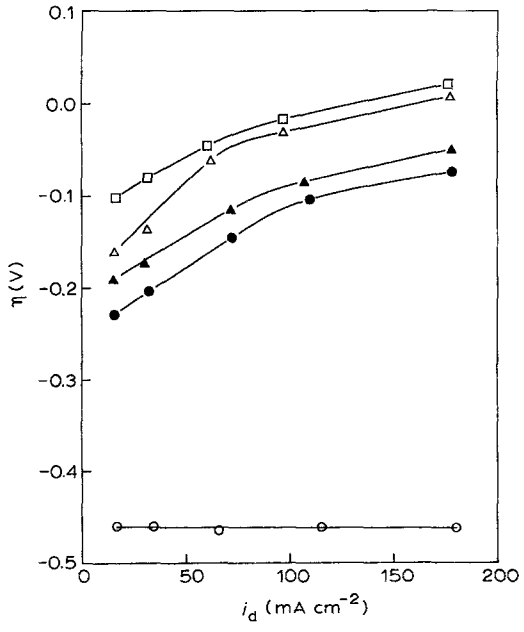

Fig. 7. Variation of the hydrogen overvoltage (η) in 1 M H_2SO_4 at 298 K with the electrodeposition current density for several electrodes. (●) $Ni2PMo_{12}$ and (▲) Ni2Mo with η at 0.5 A cm^{-2}; (○) Ni (△) $Ni2PMo_{12}$ and (□) Ni2Mo with η at 0.1 A cm^{-2}.

Table 3. Mo/Ni and P/Ni peak ratios (Pr) deduced from X-ray fluorescence spectroscopy of Ni, Ni2Mo and Ni2PMo$_{12}$ at different electrodeposition current densities (i_d)

i_d ($mA\,cm^{-2}$)	35	70	105	175
Pr (P/Ni) for Ni2Mo	5	6	6.5	7
Pr (Mo/Ni) for Ni2PMo$_{12}$	3	4.5	5	5.5

P/Ni is practically constant when i_d increases. Accordingly, the change in the h.e.r. properties on this electrode is due to the change in the Mo/Ni ratio. The non-variation of the surface area ($\sim 0{\cdot}08\ m^2\,g^{-1}$ determined by BET) of the electrode with i_d is in agreement with this interpretation. On the other hand, for different values of i_d, the variation of i_0 with $[MoO_4^{2-}]$ is shown in Fig. 8. The highest value of i_0 is obtained with Ni2Mo. Thus the different results observed here indicate that the best electrocatalytic properties are obtained on electrodes fabricated with $2\,g\,dm^{-3}$ of $PMo_{12}O_{40}^{3-}$ or MoO_4^{2-}. The variation of the Tafel slope with i_d is shown in Table 4 for Ni2PMo$_{12}$ and Ni2Mo. For both electrodes, no significant effect of i_d on b is observed. Furthermore, it may be concluded that i_d has no significant effect on the h.e.r. mechanism.

These results may be attributed to the formation of an electrocatalytic active hypo–hyper-d-electronic composite transition metal (Ni-Mo) structure. In fact, electrocatalytic activity increases sharply if the amount of Mo in the electrocatalysts is increased. Good electrocatalytic electrodes for the h.e.r. are obtained when a significant amount of molybdenum is detected in the electrocatalyst. These results may be attributed to an increase of the d-electronic density of the states at the material Fermi level. This interpretation agrees well with other published data [17, 18]. Work is currently underway to study the correlation

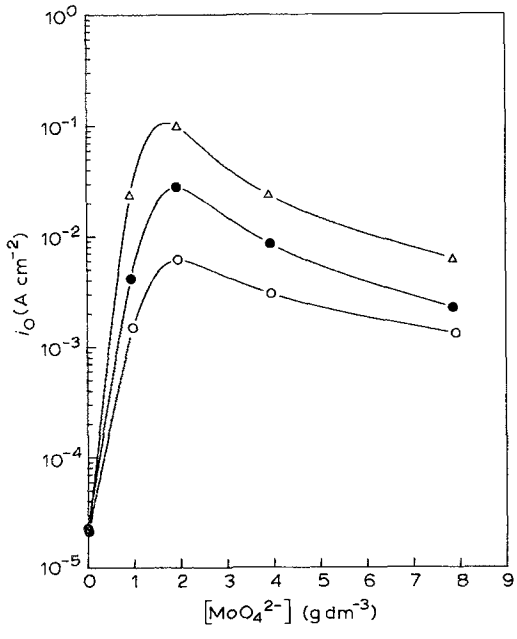

Fig. 8. Variation of the h.e.r. exchange current density in 1 M H_2SO_4 at 298 K with $[MoO_4^{2-}]$ in the electrodeposition electrolyte for different electrodeposition current densities, i_d (○) $50\,mA\,cm^{-2}$, (●) $105\,mA\,cm^{-2}$ and (△) $200\,mA\,cm^{-2}$.

Table 4. H.e.r. Tafel slope, b, at 298 K in 1 M H_2SO_4 for Ni2PMo$_{12}$ or Ni2Mo at different current densities*

i_d ($mA\,cm^{-2}$)	35	70	105	175
b (Ni2PMo$_{12}$)	90	70	70	80
b (Ni2Mo)	70	60	80	90

* b in $mV\,dec^{-1} \pm 10\,mV\,dec^{-1}$.

between the h.e.r. activity of the electrodes, their stoichiometric laves phases and their Mo content. It has been further shown that the improvement in the electrocatalytic properties for the h.e.r. on the nickel electrodeposited with $PMo_{12}O_{40}^{3-}$ or MoO_4^{2-} is mainly related to their chemical composition and not to an increase in surface area. These results are different from those obtained classically on Raney-nickel electrodes where an improvement in the h.e.r. is generally attributed to an increase of the electrode surface area ([19] and references therein).

On the other hand, the influence of the electrode activation on the h.e.r. can be determined through a study of the effect of temperature on the electrocatalytic properties of Ni2PMo$_{12}$ or Ni2Mo. The *IR* corrected current–potential curves for the h.e.r. in the case of Ni2PMo$_{12}$ or Ni2Mo in 1 M H_2SO_4 also follow typical Tafel behaviour for different experimental temperatures. The electrocatalytic activity is slightly improved by a temperature increase. As may be seen in Table 5, no evidence of a typical change in the Tafel slope was observed at high cathodic current density. The Tafel slopes are independent of temperature (b_1 and $b_2 = 80\,mV\,dec^{-1}$), which indicates that the h.e.r. mechanism does not change with an increasing temperature. Furthermore, an apparent heat of activation ΔH^* can be calculated from Equation 1 [20–25] using the temperature dependence of $\log(i_0)$ (Fig. 9).

$$\Delta H^* = -2.303R\,[\partial \log(i_0)/\partial(1/T)] \qquad (1)$$

The apparent heat of activation at reversible potential is $50\,kJ\,mol^{-1}$ for Ni [15]. This value is higher than the apparent heat of activation on Ni2PMo$_{12}$ and on Ni2Mo (Fig. 9), where the apparent heats of activation are $25\,kJ\,mol^{-1}$ and $15\,kJ\,mol^{-1}$, respectively. It should be pointed out that the apparent heats of activation on Ni2PMo$_{12}$ and on Ni2Mo were calculated using Equation 4 from Fig. 9 and the fact that the Tafel slope is temperature independent (Table 5). The

Table 5. Hydrogen Tafel slope for high current density for Ni2PMo$_{12}$ (b_1) and for Ni2Mo (b_2) at different electrolysis temperatures

Temperature (K) ±2 K	b_1 ($mV\,dec^{-1}$) ±10 mV	b_2 ($mV\,dec^{-1}$) ±0.10 mV
298	80	65
310	75	75
325	70	80
335	80	80
345	85	85
360	90	70
378	75	90

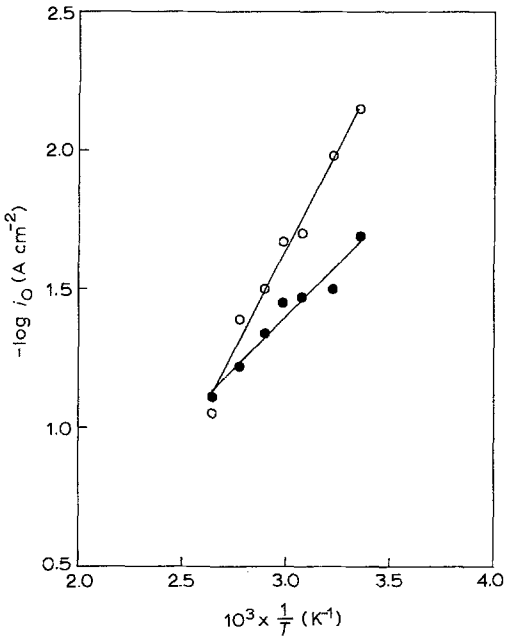

Fig. 9. Arrhenius plot of the exchange current density for the h.e.r. on (○) $Ni2PMo_{12}$ and on (●) Ni2Mo electrodeposited at 35 mA cm^{-2}.

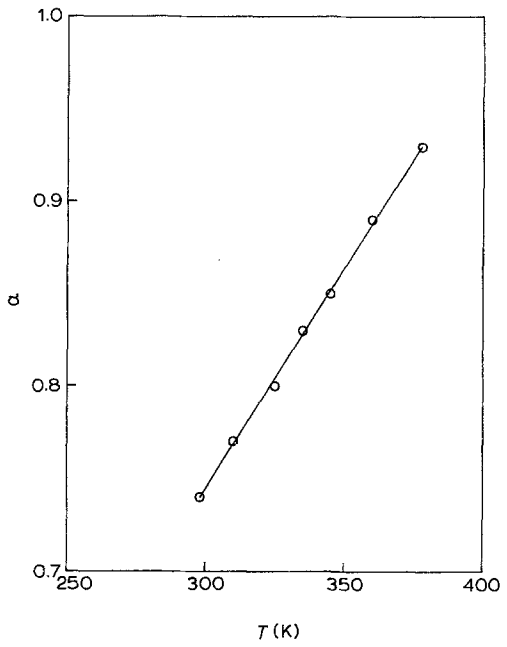

Fig. 10. Temperature dependence of the transfer coefficient for the h.e.r. on Ni2Mo electrodeposited at 35 mA cm^{-2}.

value of the heat of activation of Ni is the same as the reported values in acid solutions [14, 15] and is higher than that assumed for a Volmer rate-determining step [22]. The decrease in the apparent heats of activation on $Ni2PMo_{12}$ and Ni2Mo may be attributed to the electrode electro-activation by $PMo_{12}O_{40}^{3-}$ or MoO_4^{2-} involving active species (as described above) and, perhaps, to the corresponding electro-adsorbed hydrogen. Since the electrode activation is shown to be insufficient to modify the h.e.r. mechanism (for example, no change in the h.e.r. Tafel slope was observed), the difference may be mostly related to a change in the reaction step. The ΔH^* value on $Ni2PMo_{12}$ or Ni2Mo is less than that assumed for the Volmer step [22]. Accordingly, the Tafel step is not the rate-determining step of the h.e.r. on $Ni2PMo_{12}$ or Ni2Mo. On the other hand, the decrease in ΔH^* from 50 to 25 and thence 15 kJ could be an indication of a shift from diffusion to a mixed process of the h.e.r. The temperature independence of the Tafel slope from $b = 2.3\ RT/\alpha F$ may be attributed to a temperature dependence of the transfer coefficient (α) for the h.e.r. (Fig. 10). As may be seen, the change of α with T is linear with a slope of 0.0030 K^{-1} for $Ni2PMo_{12}$ and Ni2Mo, which is close to the value observed in the numerous cases where the Tafel slope was observed to be quasi temperature independent [23–25]. The electrode activation has no effect on this behaviour. On the other hand, the remarkable improvement in the hydrogen overvoltage (η) on the electrodes electromodified with $PMo_{12}O_{40}^{3-}$ or MoO_4^{2-} agrees well with their good electrocatalytic properties as previously shown.

Acknowledgements

The authors gratefully acknowledge the Natural Sciences and Engineering Research Council of Canada the Department of National Defence and "Le programme actions structurantes des fonds FCAR du Gouvernement du Québec" for their financial support.

References

[1] B. Keita and L. Nadjo, *J. Electroanal. Chem.* **191** (1985) 411.
[2] *Idem. ibid.* **227** (1987) 77.
[3] A. J. McEvoy and M. Gratzel, *ibid.* **209** (1986) 391.
[4] O. Savadogo, *Can. J. Chem.* **67** (1989) 382.
[5] O. Savadogo, The Proceedings of the 13th International Precious Metals Institute (IPMI), (edited by Harris, Allentown, USA (1989) 75–88.
[6] M. M. Jaksić, *Electrochem. Acta* **29** (1984) 1539.
[7] *Idem. Int. J. Hydrogen Energy* **12** (1987) 727.
[8] *Idem. J. Mol. Catalysis* **38** (1986) 161.
[9] *Idem. Mater. Chem. Phys.* **22** (1989) 1.
[10] N. Alonso-Vanté, B. Schubert and H. Tributsch, *ibid.* **22** (1989) 281.
[11] O. Savadogo and S. Thibault, *Int. J. Hydrogen Energy* **12** (1989) 865.
[12] O. Savadogo and D. L. Piron, *ibid.* **15** (1990) 715.
[13] O. Savadogo and C. Allard, *Can. Quat. Metal.*, (in press).
[14] O. Savadogo and K. Amuzgar, *Int. J. Hydrogen Energy* **15** (1990) 783.
[15] O. Savadogo and C. Allard, *J. Appl. Electrochem.*, (in press).
[16] Hailennchael Alemu and K. Juttner, *Electrochim. Acta* **33** (1988) 1101.
[17] H. Fukushima, T. Akigamo, S. Akagi and K. Higashi, *Trans. Japan Inst. Metals* **20** (1979) 358.
[18] N. Alonso Vante, B. Schubert, H. Tributsch and A. Pettin, *J. Catalysis* **112** (1988) 384.
[19] Y. Choquette, H. Ménard and L. Brossard, *Int. J. Hydrogen Energy* **15** (1990) 21.
[20] J. O'M. Brokis and E. C. Potter, *J. Chem. Phys.* **20** (1952) 247.
[21] B. E. Conway, E. M. Neatty and P. A. Demaine, *Electrochem. Acta* **7** (1962) 39.
[22] M. Enyo, *J. Electroanal. Chem.* **134** (1982) 74.
[23] E. Gileadi, *J. Electrochem. Soc.* **134** (1987) 117.
[24] B. E. Conway, D. F. Tessier and D. P. Willkinson, *J. Electroanal. Chem.* **199** (1986) 249.
[25] B. E. Conway, in 'Modern Aspects of Electrochemistry', vol. 16, (edited by B. E. Conway, R. E. White and J. O'M. Brokris), Plenum Press, New York (1985) Chap. 2.